

1 Article

2 Microwave-assisted Synthesis of Imidazole 3 [4,5f][1,10]phenanthroline Derivatives as Apoptosis 4 Inducers in Chemotherapy by Stabilizing *Bcl-2* 5 G-quadruplex DNA

6 Li Li^{1, #}, Yu-Mei Li^{1, #}, Qiong-Wu¹, Cheng-Xi Wang¹, Yong-Chang Zeng^{2,3}, Zhi-Ping Zeng¹,
7 Fen-Yong Sun^{4, *}, Wen-Jie Mei^{1, *}

8 ¹ School of Pharmacy, Guangdong Pharmaceutical University, Guangzhou, 510006, P.R. China.

9 ² Shenzhen Institute of Geriatrics, Shenzhen, 518020, P.R. China.

10 ³ The First Affiliation Hospital of Shenzhen University, Shenzhen, 518020, P.R. China.

11 ⁴ Department of Clinical Laboratory Medicine, Shanghai Tenth People's Hospital of Tongji University,
12 Shanghai, 20007, P.R. China.

13 * Correspondence: wenjiemei@126.com, Tel.: +86-13560142805; sunfenyong@263.net, Tel.: +86-18917683570

14 Academic Editor: name

15 Received: date; Accepted: date; Published: date

16 **Abstract:** Microwave-assisted synthetic technology is widely employed in synthesis for of organic
17 molecules has long been facilitated in organic synthesis to build versatile molecules in medicine.
18 Moreover, this method has received widespread attention for the controlled temperature and
19 stable condition during the reaction process. Herein, a series of imidazo [4,5f][1,10] phenanthroline
20 derivatives RPIP (PIP = imidazo [4,5f][1,10] phenanthroline, R = NO₂, 1; CF₃, 2; Cl, 3; OH, 4) have
21 been synthesized in yields of 82.3%–94.7% at 100°C under the irradiation of microwave. The
22 inhibitory activity of these compounds against various tumor cells have been investigated by MTT
23 assay. The results indicated that this class of compounds exhibited excellent inhibitory effect
24 against different tumor cells, especially for 1 inhibited the growth of A549 cells with IC₅₀ of 3.35
25 μM. The further study showed that this compound entered into tumor cells and distributed at
26 mitochondria, and then lead to tumor cells dead through induction of apoptosis. Furthermore, the
27 DNA-binding properties were investigated by spectroscopy and CD titration suggested that 1
28 could bind to *bcl-2* G-quadruplex DNA, then to interfere the Bcl-2 related apoptosis pathway. In a
29 word, 1 may act as a potential apoptosis inducer mediated-mitochondria by binding to the *bcl-2*
30 G-quadruplex DNA in cancer chemotherapy.

31 **Keywords:** Microwave-assisted synthesis; Imidazo [4,5f][1,10] phenanthroline derivatives;
32 Apoptosis inducers, *Bcl-2* G-quadruplex DNA.

33 **PACS:** J0101

34

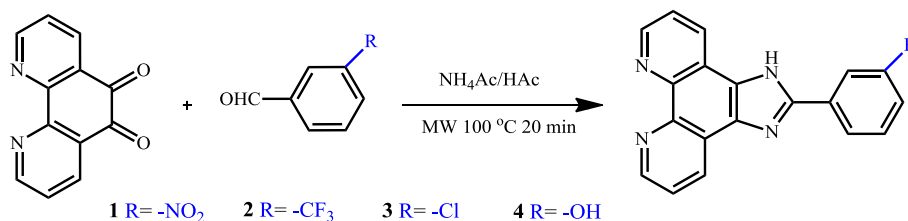
35 1. Introduction

36 1,10-Phenanthroline derivatives with an extended π -conjugated unit of fused imidazole can
37 bind to duplex DNA and G-quadruplex DNA through π - π stacking, which exhibit great antitumor,
38 anti-inflammatory and antiviral activity [1]. Furthermore, some researchers reported that
39 phenanthroline-dione derivatives might increase the chemosensitivity of esophageal cancer patients
40 to develop as a potential anticancer candidate [2]. Due to the fluorescence sensory properties
41 towards acid, phenanthroline derivatives have also been widely used as the probes of DNA [3].
42 Moreover, there is clear evidence that this type of compounds can act as antitumor agents against

43 various tumors. For example, Chunying Wei and co-workers have found that the di-substituted
 44 phenanthroline derivatives can bind to human telomeric G-quadruplexes DNA and inhibit
 45 significantly the telomerase activity resulted in tumor cells apoptosis [4, 5]. In our previous work, it
 46 has been suggested that imidazo[4,5f][1,10]phenanthroimidazole derivatives showed excellent
 47 inhibitory effect against different tumor cells, which can bind to G-quadruplex DNA in groove
 48 binding mode and block DNA replication, then induced breast cancer cells apoptosis [6, 7].

49 The *bcl-2* G-quadruplex DNA is a key director to regulate the expression of Bcl-2, a crucial
 50 member of the Bcl-2 family of proteins to accelerate the apoptosis, which may act as a potential
 51 tumor chemotherapy target. Bcl-2 protein is overexpressed in various human tumor cells [8]. More
 52 recently, a number of small molecules with ligands of highly binding ability to *bcl-2* G-quadruplex
 53 DNA have been reported that can inhibit the transcription of Bcl-2 gene and induce the tumor cells
 54 apoptosis, such as pyridostatin analog [9], metal complexes [10], quindoline derivatives [11], etc.
 55 Our group has shown phenanthroline derivatives can effectively inhibit the growth of tumor cells,
 56 which attributed to the ability to induce the cancer cells apoptosis through binding and stabilizing
 57 the G-quadruplex DNA. This work might imply this kind of compounds can also interact with the
 58 *bcl-2* G-quadruplex DNA. However, it's still not clear whether phenanthroimidazole derives can
 59 inhibit the growth of tumor cells through stabilizing the G-quadruplex structure of *bcl-2* promoter,
 60 and it's very important to design novel candidates with high activity and selectivity to tumor cells.

61 In this study, a series of imidazo [4,5f][1,10]phenanthroline derivatives have been synthesized
 62 under microwave irradiation (Scheme 1). The anti-tumor activity of these compounds against the
 63 human lung adenocarcinoma A549 cells, human hepatocarcinoma SMCC7721 cells, and human
 64 colorectal carcinoma SW620 cells were evaluated by MTT assay. The results showed this type of
 65 compounds can effectively inhibit the growth of tumor cells, especially **1** had the best inhibition
 66 activity against A549 cells. The further study displayed **1** could enter into A549 cells and be
 67 distributed at mitochondria, and inhibit the tumor cells at G1 phase then induced apoptosis. It was
 68 found that **1** exhibited some certain degree binding affinity to *bcl-2* G-quadruplex DNA, which may
 69 consider as a potential regulated role in the mechanism of this kind of compounds, resulting the
 70 tumor cells apoptosis.



71
 72 **Scheme 1.** Microwave-assisted synthesis route for phenanthroimidazole derivatives.

73 2. Results and discussion

74 2.1 Microwave-assisted synthesis of the phenanthroimidazole derivatives

75 Microwave-assisted synthesis technology has been widely developed in the fields of chemical
 76 synthesis, materials science, and biotechnology [12, 13]. The technique observably shorten reaction
 77 time, while increasing yield and product purity over traditional synthesis methods, especially in the
 78 synthesis of organic molecules which typically require long hours of heating at reflux in
 79 high-boiling solvents to affect a reaction [14]. As shown in Figure 1, the reaction temperature
 80 rapidly reached setting value less than 60 s, and kept great stabilization and homogeneous of
 81 temperature and pressure in the whole heating process. As a result, the yields of the target
 82 compounds increased obviously in far more less times than conventional heating methods. These
 83 results suggested the application of microwave irradiation has significantly increased the yields for
 84 most of the compounds to about 90%, which were much higher than those of conventional
 85 synthesis methods [15].

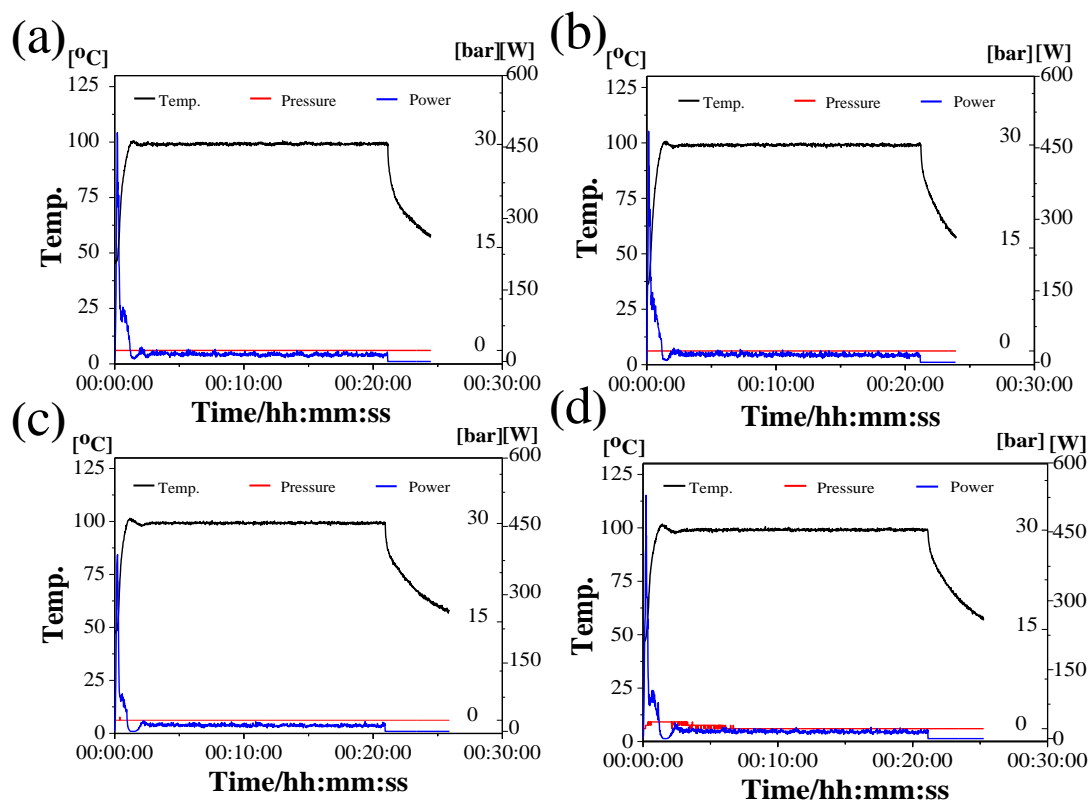


Figure 1. Reaction profile of the target complexes in glacial acetic acid irradiated by microwave for 20 min at 100°C, (a) 1; (b) 2; (c) 3; (d) 4.

Table 1. The yields of the target complexes by microwave-assisted synthesis method.

Compd.	Microwave-Assisted		
	Temperature/°C	Time/min	Yield%
1	100	20	91.3%
2	100	20	82.3%
3	100	20	94.7%
4	100	20	89.7%

2.2 Biological activity

The synthetic phenanthroimidazole derivatives can effectively inhibit the human lung adenocarcinoma A549 cells, human hepatocarcinoma SMCC7721 cells, and human colorectal carcinoma SW620 cells growth and proliferation, which were confirmed by MTT assay. *Cis*-platin was used as a positive control, and the inhibitory activities (IC_{50}) of these complexes were listed in Table 2. It was observed that these compounds displayed great growth inhibition against various tumor cells after 72 h treatment, especially the inhibitory activity (IC_{50}) of **1** against A549 cells was about 3.35 μ M, which was far more less to that of *cis*-platin (16.54 μ M). The data suggested that phenanthroimidazole derivatives blocked the growth of tumors cells, and those derivatives with electron-withdrawing meta-substituents, the complex with $-NO_2$ substitution exhibited higher anti-tumor activity against A549 cells than that of the complex with $-CF_3$ substituent, as to electron-donating meta-substituents, the complex with $-Cl$ substitution had higher inhibitory activities of A549 tumors cells than that of the complex with $-OH$ substituent.

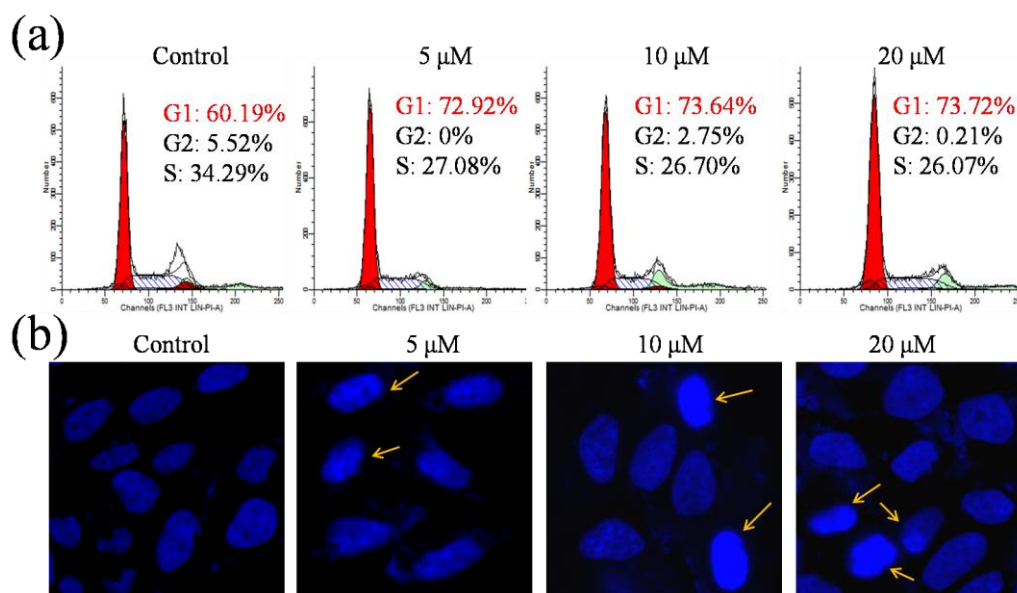
Table 2. The inhibitory effect IC_{50} (μ M) of the target complexes and *cis*-platin on human cancer cells

Compd.	IC ₅₀ (μM)		
	A549	SMMC-7721	SW620
1	3.35	> 100	4.53
2	11.23	22.34	10.32
3	4.16	15.39	10.52
4	8.36	11.28	7.52
cis-platin	16.54	2.92	5.74

105

106 2.3 Apoptosis induction

107 According to the above results of the MTT assay, **1** showed great inhibitory activity against A549
108 cells comparing with the other compounds. Apoptosis and cell cycle arrest, or a combined action of
109 both can result in growth inhibition or death of cells [16]. Thus, to further understand the
110 underlying mechanisms of **1**, flow cytometric analysis was carried out. The A549 cells were exposed
111 to different concentrations of **1** (0, 5, 10, and 20 μM) and showed a significant increase G1-phase
112 arrest for 24 h (Figure 2a), upon the increasing concentration of **1**, the ratio of cell G1-phase arrest
113 increased markedly, even reached about 73.72% for the 20 μM target compound, which was
114 approximately a quarter higher than that of the control (60.19%). Owing to G1 phase arrest is more
115 related cell apoptosis [17, 18], Hoechst 33258 dye cell nucleus was used to observe cell apoptosis. It
116 was found that, with the increasing of **1**, the cell nucleus shrink obviously and highlight markedly,
117 which is the marker of apoptosis (Figure 2b). The observations indicated that **1** may induce A549
118 cells G1-phase arrest then resulted in apoptosis.



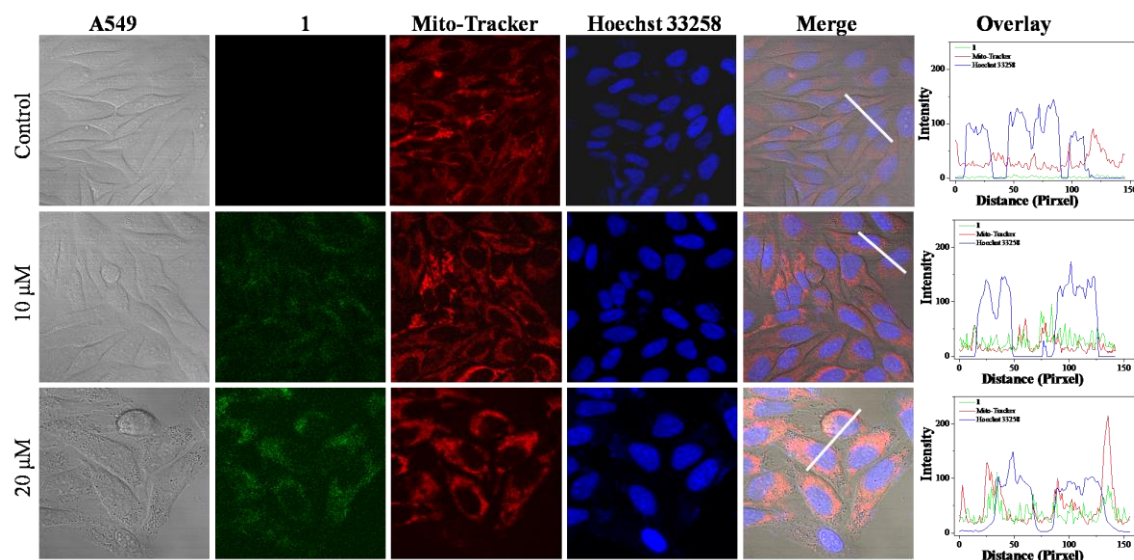
119

120 **Figure 2.** (a) G1-phase arrest of A549 cells induced by **1**. A549 cells were treated with **1** (0, 5, 10, and
121 20 μM) for 24 h, almost 73% cycling cells were in the G1-phase and the sharp peak suggested that some
122 cells were experiencing G1-phase delay or arrest. (b) Induction of cells apoptosis of **1** by Hoechst 33258
123 dye. A549 cells were dyed with Hoechst 33258 at different concentrations of **1** (0, 5, 10, and 20 μM) for 24
124 h.

125 2.4 Drug distribution and location

126 Cellular localization of **1** in A549 cells was further investigated, as shown in Figure 3. It was
127 observed that **1** can be uptook by A549 cells and glow weak green fluorescence, a possible reason is

128 mainly due to the absence of hypochrome nitro-group. Here, the mitochondria were marked in red
 129 by Mito-tracker, and the nuclei of A549 cells were stained blue by Hoechst 33258. Upon the
 130 addition of **1**, an increasing green fluorescence was great merged with red fluorescence in the cell
 131 mitochondria, but little overlay in cell nucleus. These results indicated this compound entered into
 132 cells majorly accumulated in the mitochondria of A549 cells, which may induce the cell apoptosis
 133 through mitochondria-mediated pathway.



134

135 **Figure 3.** Cellular localization of **1** in A549 cells. Cells were treated with the **1** for 6 h at 37 °C: blue, Hoechst
 136 33258; red, Mito-Tracker . [1] = 0, 10 and 20 μM. The overlay data were analyzed using Image Pro Plus.

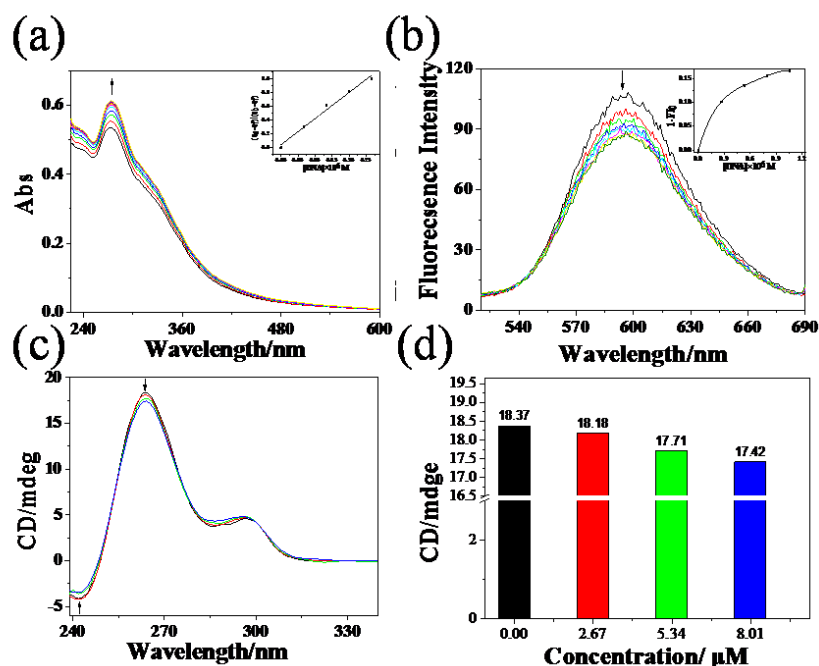
137 2.5 The interaction of *Bcl-2* G-quadruplex DNA with phenanthroimidazole derivatives

138 2.5.1 Electronic titrations

139 UV absorption was carried out to monitor the interaction of **1** with *bcl-2* G-quadruplex DNA.
 140 As shown in Figure 4a, the electronic spectra of **1** in Tris-HCl buffer (pH = 7.4) solution exhibited
 141 the characteristic IL (intraligand charge transfer) absorption in the range of 250–300 nm with the
 142 maximum at about 273 nm. When the DNA was gradually added to the solution of the complex, a
 143 hyperchromic effect and a bathochromic effect were observed. The hyperchromism value of **1** at the
 144 IL absorption band was about 14.1% ($\Delta\lambda = 2.1$ nm), which may be attributed to bases of the DNA
 145 exposed, when the ligand binding to DNA, induced external contact or to partial uncoiling of the
 146 DNA structure [19, 20]. Furthermore, the value of the intrinsic binding constant (K_b) for **1** was about
 147 $8.7 \times 10^7 \text{ M}^{-1}$, calculated according to the decay of IL absorption. These data implied that **1** bound to
 148 *bcl-2* G-quadruplex DNA with high affinity in intercalating mode [21]. The interaction was further
 149 confirmed by the following fluorescence quenching experiment.

150 2.5.2 Fluorescence quenching

151 Because of the low fluorescence of **1** in the Tris-HCl KCl buffer (PH = 7.4), fluorescence
 152 quenching of ethidium bromide (EB) and DNA was carried out. As shown in Figure 4b, when
 153 excited at 350 nm, the EB-DNA (*bcl-2* G4 DNA) solution emitted a strong fluorescence in the range of
 154 500 to 700 nm with the maximum at about 597 nm [22]. Upon the **1** added into solution, it was
 155 observed the fluorescence intensity of the solution decreased gradually, which suggested that **1** can
 156 competitive association with *bcl-2* G-quadruplex DNA. At [Compd.] = 20.89 μM, the relative
 157 intensity (I/I_0) for solution DNA was about 0.83. The results implied that **1** exhibited a certain interaction
 158 with *bcl-2* G-quadruplex DNA.



159

160 **Figure 4.** The study of the interaction between **1** with *bcl-2* G-quadruplex DNA by spectroscopic methods.
 161 **(a)** The electronic spectra of **1** in absence and in presence of *bcl-2* G-quadruplex DNA. [**1**] = 60 μM , [DNA] =
 162 100 μM . **(b)** Emission spectra of EB and *bcl-2* G-quadruplex DNA in the incubation buffer in the absence
 163 and presence of **1**, [EB] = 16 μM , [DNA] = 2 μM . **(c)** CD titration spectra of *bcl-2* G-quadruplex DNA at
 164 different concentrations of **1**, ([**1**] = 0, 2.66, 5.305, 7.937 μM). **(d)** The change of CD signal at 263 nm of *bcl-2*
 165 G-quadruplex DNA with the addition of **1** in the Tris-HCl buffer.

166 2.5.3 Circular dichroism spectra

167 CD spectra is one of the most common and convenient methods for detecting DNA
 168 conformational changes. CD titration experiment was further carried out to confirm the binding of **1**
 169 with *bcl-2* G-quadruplex DNA, and the results were shown in Figure 4c. The CD spectra of *bcl-2*
 170 G-quadruplex DNA displayed a positive CD signal between 250 and 300 nm with the maximum at
 171 264 nm, which was the characteristic CD signal of G4 DNA, in addition to a weak negative CD
 172 signal in the range of 200-250 nm with the maximum at 245 nm [23]. Upon the addition of **1**, the
 173 positive signal of *bcl-2* G-quadruplex DNA in the CD spectra were decreased, the strength of the
 174 positive CD signal (263 nm) and the negative CD signal (245 nm) decreased by 5.6% and 15.2%,
 175 respectively. These data indicated that the ligand can stabilize and bind to the *bcl-2* G-quadruplex
 176 DNA.

177 3. Conclusions

178 In summary, a series of phenanthroimidazole derivatives have been synthesized by using
 179 microwave-assisted synthesis technology, with high yields of approximately 90%, which can rapid
 180 rising to the required temperature, and kept almost no change during the whole process. The results
 181 of MTT assay showed these complexes can block the growth of tumor cells, especially **1**, exhibited
 182 excellent antitumor activity against A549 cells through inducing apoptosis of the cells. The further
 183 study displayed **1** can distribute at mitochondria, and inhibit tumor cells at G1 phase then induce
 184 apoptosis. Furthermore, the investigation by spectroscopy and CD titration demonstrated that this
 185 compound can bind to the *bcl-2* G-quadruplex DNA. Take together, this type of
 186 phenanthroimidazole derivatives can act as potential antitumor agents targeting to the *bcl-2*
 187 G-quadruplex DNA in cancer chemotherapy.

188

189

190 4. Experimental Section

191 4.1 Materials

192 All reagents were purchased from commercial suppliers and used without further purification.
193 Solvents were dried and purified by conventional methods prior to use. Distilled water was used in
194 all experiments. *bcl-2* G-quadruplex DNA (5'-CGGGCGCGGGAGGAAGGGGGCGGGAGC-3') was
195 purchased from Sangon Biotech and formed a G-quadruplex conformation as literature by
196 renaturation for 24 h at 4°C, after denaturation for 5 min at 90°C [24]. All aqueous solutions were
197 prepared with doubly distilled water. The Tris-HCl buffer consisting of Tris and KCl, and the pH
198 value was adjusted to 7.4 by HCl solution, which was applied to UV titration and Fluorescence
199 emission titrations.

200 4.2 Instruments

201 The phenanthroimidazole derivatives were synthesized by using Anton Paar Monowave 300
202 microwave reactor. ESI-MS spectra were obtained in methanol on Agilent 1100 ESI-MS system
203 operating at room temperature. The ¹H NMR and ¹³C NMR spectra were recorded in a dimethyl-*d*⁶
204 sulfoxide (DMSO-*d*⁶) solution on a Bruker Avance III 500 spectrometer operating at room
205 temperature. UV-vis absorption spectra were recorded on a Shimadzu UV-2550 spectrophotometer.
206 The steady-state emission spectra were recorded on a RF-5301 fluorescence spectrophotometer.

207 4.3 Synthesis of imidazole[4,5*f*][1,10] phenanthroline derivatives

208 Phenanthroimidazole derivatives were synthesized according to the literature procedure with
209 some modification [8].

210 4.3.1 Synthesis of compound 1.

211 A mixture of 1,10-phenanthroline-5,6-dione (315.06 mg, 1.50 mmol), 3-nitrobenzaldehyde
212 (339.81 mg, 2.25 mmol), ammonium acetate (4 g, 51.9 mmol) and glacial acetic acid (20 mL) was
213 heated at 100 °C for 20 min under microwave irradiation. Then, 20 ml of water was added and the
214 pH value was adjusted to 7.0 at room temperature. The solution was filtered and dried
215 in vacuum to obtain a yellow precipitate, which was collected and washed with water and small
216 amounts of ethanol. The crude product dissolved in ethanol was purified by filtration on silicagel
217 column (60–100 mesh). ESI-MS (in MeOH, *m/z*): 342.1 [M+H]⁺. ¹H NMR (500 MHz, DMSO) δ 9.03 –
218 9.02 (m, 1H), 9.00 (dd, *J* = 4.3, 1.7 Hz, 2H), 8.84 (dd, *J* = 8.1, 1.7 Hz, 2H), 8.64 (d, *J* = 8.0 Hz, 1H), 8.27
219 (dd, *J* = 8.1, 1.5 Hz, 1H), 7.83 (t, *J* = 8.0 Hz, 1H), 7.78 (dd, *J* = 8.1, 4.3 Hz, 2H). ¹³C NMR (126 MHz,
220 DMSO) δ 150.38 (s), 145.70 (s), 134.14 (s), 132.63 (s), 131.70 (s), 125.58 (s), 125.29 (s), 122.30 (s).

221 4.3.2 Synthesis of compound 2.

222 **2** was prepared using the method described above, but with 3-trifluoromethylbenzaldehyde
223 (391.5 mg, 2.25 mmol). ESI-MS (in MeOH, *m/z*): 365.5 [M+H]⁺. ¹H NMR (500 MHz, DMSO) δ 9.00
224 (dd, *J* = 4.3, 1.7 Hz, 1H), 8.84 (dd, *J* = 8.1, 1.6 Hz, 1H), 8.55 (s, 1H), 8.53 (d, *J* = 7.3 Hz, 1H), 7.85 – 7.81
225 (m, 1H), 7.78 (dd, *J* = 8.1, 4.3 Hz, 1H). ¹³C NMR (126 MHz, DMSO) δ 150.88 (s), 149.99 (s), 145.75 (s),
226 133.03 (s), 132.29 (s), 131.98 (s), 131.64 (s), 125.30 (s).

227 4.3.3 Synthesis of compound 3.

228 **3** was prepared using the method described above, but with 3-chlorobenzaldehyde (315 mg,
229 2.25 mmol). ESI-MS (in MeOH, *m/z*): 331.3 [M+H]⁺. ¹H NMR (500 MHz, MeOD:CDCl₃ = 1:1) δ 8.95 –
230 8.89 (m, 2H), 8.79 (s, 1H), 7.99 (t, *J* = 9.4 Hz, 2H), 7.62 (s, 2H), 7.57 (s, 1H), 7.29 (t, *J* = 8.7 Hz, 2H). ¹³C

231 NMR (126 MHz, MeOD:CDCl₃ = 1:1) δ 149.06 (s), 144.91 (s), 141.69 (s), 131.63 – 131.46 (m), 131.08 (s),
232 127.96 (s), 124.76 (s).

233 4.3.4 Synthesis of compound 4.

234 4 was prepared using the method described above, but with 3-Hydroxybenzaldehyde (274.59
235 mg, 2.25 mmol). ESI-MS (in MeOH, m/z): 313.1 [M+H]⁺. ¹H NMR (500 MHz, DMSO) δ 9.02 (dd, *J* =
236 4.3, 1.7 Hz, 2H), 8.91 (dd, *J* = 8.1, 1.7 Hz, 2H), 7.81 (dd, *J* = 8.1, 4.3 Hz, 2H), 7.73 (dd, *J* = 6.0, 3.8 Hz,
237 1H), 7.72 – 7.69 (m, 1H), 7.39 (t, *J* = 7.9 Hz, 1H), 6.91 (ddd, *J* = 8.1, 2.4, 0.8 Hz, 1H). ¹³C NMR (126
238 MHz, DMSO) δ 152.95 (s), 149.75 (s), 145.55 (s), 133.43 (s), 132.07 (s), 131.68 (s), 125.30 (s), 119.07 (s),
239 118.72 (s), 115.16 (s).

240 4.4 Cell Lines, Cell Culture and MTT Assay

241 Human cancer cell lines, human lung adenocarcinoma A549 cells, human hepatocarcinoma
242 SMMC7721 cells, and human colorectal carcinoma SW620 cells were purchased from American
243 Type Culture Collection (ATCC, Manassas, VA, USA). All cell lines were maintained in Dulbecco's
244 Modified Eagle Medium (DMEM) media supplemented with fetal bovine serum (10%), penicillin
245 (100 units/mL), and streptomycin (50 units/mL) at 37 °C in a CO₂ incubator (95% relative humidity,
246 5% CO₂).

247 Cell viability was confirmed by measuring the ability of cells to transform
248 3-(4,5-dimethylthiazol-2-yl)-2,5-diphenyltetrazolium bromide (MTT) to a purple formazan dye [25].
249 Cells were seeded in 96-well tissue culture plates (3 × 10³ cells per well) for 24 h. The cells were then
250 incubated with the tested compounds at different concentrations for 72h. After incubation, 20 μL
251 per well of MTT solution (5 mg/mL in phosphate buffered saline, PBS) was added, followed by
252 incubation for a further 5 h. The medium was aspirated and replaced with 150 μL/well of DMSO to
253 dissolve the formazan salt formed. The colour intensity, which reflects the cell growth condition,
254 was measured at 570 nm using a microplate spectrophotometer (SpectroAmax™250, BioTek
255 Instruments, Inc., Winooski, VT, USA)

256 4.5 Flow Cytometric Analysis

257 The apoptosis rate was analysed by flow cytometry. Treated or
258 untreated cells were trypsinised, washed with PBS, and then fixed in 75% ethanol overnight at -20 °C.
259 Next, the fixed cells were washed with PBS and stained with propidium iodide (PI) for 4 h in the
260 dark. Finally, the above-described cells were analyzed with an Epics XL-MCL flow cytometer
261 (Beckman Coulter, Miami, FL, USA).

262 4.6 Cellular localization

263 Cells were cultured in DMEM medium supplemented with 10% fetal bovine serum (FBS) at
264 37 °C under 5% CO₂. Cells in complete growth medium at 2 × 10⁶ cells per mL were incubated for 6h
265 at 37°C, unless otherwise stated. Cells were washed with PBS and then treated with 1 in DMSO/PBS
266 (pH 7.2, 1 : 99, v/v) for 2 h at 37 °C under 5% CO₂. Then, cells were stained with Mito-tracker and
267 Hoechst 33258 for another 20 min, and finally, luminescence imaging was carried out by confocal
268 microscopy.

269 4.7 Electronic absorption measurements

270 Electronic absorption spectra were recorded on a Shimadzu UV-2550 spectrophotometer using
271 1 cm path length quartz cuvettes (3 mL). The absorption titration of the target complexes in Tris-HCl
272 buffer was performed by using a fixed complex concentration to which increments of the DNA
273 stock solution were added. The concentration of the complex solution was 20 μM and *bcl-2* G4 DNA

274 was added by degrees. Complex-DNA solutions were allowed to incubate for 3 min before the
275 absorption spectra were recorded.

276 4.8 Fluorescence quenching measurements

277 Fluorescence spectroscopy measurements were performed on a RF-5301 fluorescence
278 spectrophotometer using a 1 cm path length quartz cell. Fluorescence quenching of the EB + *bcl-2*
279 G4 DNA system can be used for a compound having an affinity to DNA in spite of its binding
280 mode, and only measures the ability of the compound to affect the EB fluorescence intensities in the
281 EB + *bcl-2* G4 DNA system. The titration processes were repeated until there was no apparent
282 change in the spectra for at least three titrations, indicating the achievement of the binding
283 saturation [26].

284 4.9 CD spectra measurements

285 CD spectra were recorded on a Jasco J810 circular dichroism (CD) spectrophotometer with a
286 thermoelectrically controlled cell holder. The cell path length was 1 cm. CD spectra were recorded
287 in the range of 230-600 nm in 0.5 nm increments with an averaging time of 0.5 s [27].

288 **Acknowledgments:** This work was supported by the National Nature Science Foundation of China (81572926),
289 the Provincial Major Scientific Research Projects in Universities of Guangdong Province (2014KZDXM053), the
290 Science and Technology Project of Guangdong Province (2014A020212312).

291 **Author Contributions:** Li Li contributes to electronic spectra titration, emission spectra, CD spectra titration
292 and writes the paper. Yu-Mei Li and Yong-Chang Zeng contributes to the synthesis of the target complexes;
293 Cheng-Xi Wang, Qiong-Wu and Zhi-Ping Zeng contribute to the cells experiments. Fen-Yong Sun and Wen-Jie
294 Mei contributed to designed the experiments and read the manuscript.

295 References

- 296 1. De Cian, A.; Delemos, E.; Mergny, J. L.; Teulade-Fichou, M. P.; Monchaud, D., Highly efficient
297 G-quadruplex recognition by bisquinolinium compounds. *J. Am. Chem. Soc.* **2007**, *129*, 1856-1857.
- 298 2. Zhen, N.; Yang, Q.; Zheng, K.; Han, Z.; Sun, F.; Mei, W.; Yu, Y., MiroRNA-127-3p targets XRCC3 to
299 enhance the chemosensitivity of esophageal cancer cells to a novel phenanthroline-dione derivative.
300 *Int. J. Biochem. Cell. B.* **2016**, *79*, 158-167.
- 301 3. Peng, J.; Sun, J.; Gong, P.; Xue, P.; Zhang, Z.; Zhang, G.; Lu, R., Luminescent Nanofibers Fabricated
302 from Phenanthroimidazole Derivatives by Organogelation: Fluorescence Response towards Acid with
303 High Performance. *Chem-Asian. J.* **2015**, *10*, 1717-1724.
- 304 4. Wang, L.; Wen, Y.; Liu, J.; Zhou, J.; Li, C.; Wei, C., Promoting the formation and stabilization of
305 human telomeric G-quadruplex DNA, inhibition of telomerase and cytotoxicity by phenanthroline
306 derivatives. *Org. Biomol. Chem.* **2011**, *9*, 2648-2653.
- 307 5. Wei, C. Y.; Wang, J. H.; Wen, Y.; Liu, J.; Wang, L. H.,
308 4-(1H-imidazo[4,5-f]-1,10-phenanthrolin-2-yl)phenol-based G-quadruplex DNA binding agents:
309 telomerase inhibition, cytotoxicity and DNA-binding studies. *Bioorg. Med. Chem.* **2013**, *21*, 3379-3387.
- 310 6. Liao, S.; Zhang, Z.; Wu, Q.; Wang, X.; Mei, W., Microwave-assisted synthesis of phenanthroimidazole
311 derivatives as stabilizer of c-myc G-quadruplex DNA. *Bioorg. Mei. Chemist.* **2014**, *22*, 6503-6508.
- 312 7. Zhen, N.; Yang, Q.; Wu, Q.; Zhu, X.; Wang, Y.; Sun, F.; Mei, W.; Yu, Y., A novel synthesized
313 phenanthroline derivative is a promising DNA-damaging anticancer agent inhibiting G1/S checkpoint
314 transition and inducing cell apoptosis in cancer cells. *Cancer Chemoth. Pharm.* **2016**, *77*, 169-180.
- 315 8. Wang, C.; Yu, Q.; Yang, L.; Liu, Y.; Sun, D.; Huang, Y.; Zhou, Y.; Zhang, Q.; Liu, J., Ruthenium (II)
316 polypyridyl complexes stabilize the *bcl-2* promoter quadruplex and induce apoptosis of HeLa tumor
317 cells. *Biometals* **2013**, *26*, 387-402.

- 318 9. Feng, Y.; Yang, D.; Chen, H.; Cheng, W.; Wang, L.; Sun, H.; Tang, Y., Stabilization of G-quadruplex
319 DNA and inhibition of Bcl-2 expression by a pyridostatin analog. *Bioorg. Med. Chem. Lett.* **2016**, *26*,
320 1660-1663.
- 321 10. Chen, Z. F.; Qin, Q. P.; Qin, J. L.; Liu, Y. C.; Huang, K. B.; Li, Y. L.; Meng, T.; Zhang, G. H.; Peng, Y.;
322 Luo, X. J.; Liang, H., Stabilization of G-quadruplex DNA, inhibition of telomerase activity, and tumor
323 cell apoptosis by organoplatinum(II) complexes with oxoisoaporphine. *J. Med. Chem.* **2015**, *58*,
324 2159-2179.
- 325 11. Wang, X. D.; Ou, T. M.; Lu, Y. J.; Li, Z.; Xu, Z.; Xi, C.; Tan, J. H.; Huang, S. L.; An, L. K.; Li, D.; Gu, L.
326 Q.; Huang, Z. S., Turning off transcription of the bcl-2 gene by stabilizing the bcl-2 promoter
327 quadruplex with quindoline derivatives. *J. Med. Chem.* **2010**, *53*, 4390-4398.
- 328 12. Kitchen, H. J.; Vallance, S. R.; Kennedy, J. L.; Tapia-Ruiz, N.; Carassiti, L.; Harrison, A.; Whittaker, A.
329 G.; Drysdale, T. D.; Kingman, S. W.; Gregory, D. H., Modern microwave methods in solid-state
330 inorganic materials chemistry: from fundamentals to manufacturing. *Chem. Rev.* **2014**, *114*, 1170-1206.
- 331 13. de la Hoz, A.; Diaz-Ortiz, A.; Moreno, A., Microwaves in organic synthesis. Thermal and non-thermal
332 microwave effects. *Chem. Soc. Rev.* **2005**, *34*, 164-178.
- 333 14. Beckford, F. A.; Shalowski, M.; Leblanc, G.; Thessing, J.; Lewis-Alleyne, L. C.; Holder, A. A.; Li, L.;
334 Seeram, N. P., Microwave synthesis of mixed ligand diimine-thiosemicarbazone complexes of
335 ruthenium(II): biophysical reactivity and cytotoxicity. *Dalton trans.* **2009**, 10757-10764.
- 336 15. Sun, D.-d.; Wang, W.-z.; Mao, J.-w.; Mei, W.-j.; Liu, J., Imidazo [4,5f][1,10] phenanthroline derivatives
337 as inhibitor of c-myc gene expression in A549 cells via NF- κ B pathway. *Bioorg. Med. Chem. Lett.* **2012**,
338 *22*, 102-105.
- 339 16. Xiao, H.; Zhang, Q.; Lin, Y.; Reddy, B. S.; Yang, C. S., Combination of atorvastatin and celecoxib
340 synergistically induces cell cycle arrest and apoptosis in colon cancer cells. *Int. J. Cancer.* **2008**, *122*,
341 2115-2124.
- 342 17. Wang, T.; Gong, X.; Jiang, R.; Li, H.; Du, W.; Kuang, G., Ferulic acid inhibits proliferation and promotes
343 apoptosis via blockage of PI3K/Akt pathway in osteosarcoma cell. *Am. J. Transl. Res.* **2016**, *8*, 968-980.
- 344 18. Guo, Y. X.; Lin, Z. M.; Wang, M. J.; Dong, Y. W.; Niu, H. M.; Young, C. Y.; Lou, H. X.; Yuan, H. Q.,
345 Jungermannone A and B induce ROS- and cell cycle-dependent apoptosis in prostate cancer cells in
346 vitro. *Acta Pharmacol. Sin.* **2016**, *37*, 814-24.
- 347 19. Bhattacharjee, S.; Chakraborty, S.; Sengupta, P. K.; Bhowmik, S., Exploring the Interactions of the
348 Dietary Plant Flavonoids Fisetin and Naringenin with G-Quadruplex and Duplex DNA, Showing
349 Contrasting Binding Behavior: Spectroscopic and Molecular Modeling Approaches. *J. Phys. chem. B*
350 **2016**, *120*, 8942-8952.
- 351 20. Buraka, E.; Chen, C. Y.; Gavare, M.; Grube, M.; Makarenkova, G.; Nikolajeva, V.; Bisenieks, I.; Bruvere,
352 I.; Bisenieks, E.; Duburs, G.; Sjakste, N., DNA-binding studies of AV-153, an antimutagenic and DNA
353 repair-stimulating derivative of 1,4-dihydropyridine. *Chem-Biol. Interac.* **2014**, *220*, 200-207.
- 354 21. Jager, K.; Bats, J. W.; Ihmels, H.; Granzhan, A.; Uebach, S.; Patrick, B. O., Polycyclic azoniaheterenes:
355 assessing the binding parameters of complexes between unsubstituted ligands and G-quadruplex
356 DNA. *Chemistry* **2012**, *18*, 10903-10915.
- 357 22. Wu, Q.; Chen, T.; Zhang, Z.; Liao, S.; Wu, X.; Wu, J.; Mei, W.; Chen, Y.; Wu, W.; Zeng, L.; Zheng, W.,
358 Microwave-assisted synthesis of arene ruthenium(II) complexes $[(\eta^6\text{-RC}_6\text{H}_5)\text{Ru}(\text{m-MOPIP})\text{Cl}]\text{Cl}$ (R =
359 -H and -CH₃) as groove binder to c-myc G4 DNA. *Dalton. Trans.* **2014**, *43*, 9216-9225.

- 360 23. Pany, S. P.; Bommiseti, P.; Diveshkumar, K. V.; Pradeepkumar, P. I., Benzothiazole hydrazones of
361 furylbenzamides preferentially stabilize c-MYC and c-KIT1 promoter G-quadruplex DNAs. *Org.*
362 *Biomol. Chem.* **2016**, *14*, 5779-5793.
- 363 24. Chan, D. S.-H.; Yang, H.; Kwan, M. H.-T.; Cheng, Z.; Lee, P.; Bai, L.-P.; Jiang, Z.-H.; Wong, C.-Y.;
364 Fong, W.-F.; Leung, C.-H.; Ma, D.-L., Structure-based optimization of FDA-approved drug methylene
365 blue as a *c-myc* G-quadruplex DNA stabilizer. *Biochimie* **2011**, *93*, 1055-1064.
- 366 25. Chen, T.; Wong, Y. S., Selenocystine induces reactive oxygen species-mediated apoptosis in human
367 cancer cells. *Biomed. Pharmacother.* **2009**, *63*, 105-113
- 368 26. Lu, X.-H.; Shi, S.; Yao, J.-L.; Gao, X.; Huang, H.-L.; Yao, T.-M., Two structurally analogous ruthenium
369 complexes as naked-eye and reversible molecular "light switch" for G-quadruplex DNA. *J. Inorg.*
370 *Biochem.* **2014**, *140*, 64-71.
- 371 27. Gray, D. M.; Wen, J.-D.; Gray, C. W.; Repges, R.; Repges, C.; Raabe, G.; Fleischhauer, J., Measured and
372 calculated CD spectra of G-quartets stacked with the same or opposite polarities. *Chirality* **2008**, *20*,
373 431-440.